JOURNAL OF EXPERIMENTAL AND THEORETICAL PHYSICS, 2024, Vol. 165, No. 1, pp. 47–60

GaP_xAs_{1-x} SOLID SOLUTION MBE ON (001) VICINAL SUBSTRATES: KINETIC MODEL FOR COMPOSITION FORMATION IN THE ANIONIC SUBLATTICE

© 2024 M. A. Putyato*, E. A. Emelyanov, M. O. Petrushkov, A. V. Vasev, B. R. Semyagin, V. V. Preobrazhensky

Rzhanov Institute of Semiconductor Physics
Siberian Branch of the Russian Academy of Sciences
Novosibirsk, 630090, Russia
**e-mail: e2a@isp.nsc.ru*

Received February 12, 2022
Revised April 12, 2023
Accepted April 12, 2023

Abstract. Kinetic model for composition formation in the anionic sublattice of the GaP_xAs_{1-x} solid solution during MBE on the (001) vicinal surface from As_2 and P_2 beam is proposed. The model was based on a two-dimensional layered growth mechanism according to which terraces with a reconstructed surface are successively build up in growth areas localized in step kinks. The elementary mass transfer processes in the growth areas, on the terrace surfaces and their edges were considered. The model kinetic constants were determined by comparing the calculated values of x with experimental data. The impact of the substrate temperature, growth rate, and surface misorientation angle value on the solid solution composition is explained by exchange processes in the anionic layer on the surface and edges of terraces located outside growth areas.

Keywords: *molecular beam epitaxy, $A^{III}B^V$, solid solutions, GaP_xAs_{1-x}, kinetic model*

DOI: 10.31857/S00444510240106e5

1. INTRODUCTION

Solid solutions of $A^{III}B^V$ compounds are zone engineering materials with a wide range of possible applications. On their basis, instrument heterostructures and objects for fundamental research are created. One of the main ways of forming thin-film heterostructures based on solid solutions of $A^{III}B^V$ compounds is molecular beam epitaxy (MBE). In the case of growing layers of solid substitution solutions according to the fifth group using this method, difficulties arise due to the fact that the composition in the anionic sublattice depends on the substrate temperature (T_s), molecular fluxes density, growth rate (V_g), orientation and superstructural state of the surface, as well as the molecular form of the fifth group elements. The same parameters control the properties and quality of epitaxial layers and heterojunctions. Therefore, it is necessary to coordinate the growth conditions necessary for the formation of a given composition with the growth conditions that provide the required structural, electrophysical and optical properties of the solid solution layers. For growing of heterostructures based on $A^{III}B^V$ compounds by the MBE method, substrates with a small angle of deviation from the singular face (001) ($\alpha \leqslant 0.5°$) are mainly used. This is due to the physico- chemical and technological properties of this surface. But in some cases, to suppress the processes of segregation and the development of morphology (roughness) of the surface, substrates are used that are deflected to the face (111) by an angle of more than 2° [1, 2].

Research works aimed at creating a technology for growing epitaxial heterostructures based on $A^{III}B^V$ compounds on Si(001) substrates are also actively underway. The interest in this topic is due to the prospects of monolithic integration of the $A^{III}B^V$ optoelectronic element base and silicon electronics. For a number of reasons, epitaxy of $A^{III}B^V$ on Si is performed, including on substrates deviated from the face (001) to (111) by 2° or more [3]. In [4], the results of a study of the effect of substrate misorientation on the composition of $GaAs_1-_xSb_x$ (001) films are presented. It was shown that the composition of the solid solution depends on the magnitude

of the misorientation angle, which is one of the growth parameters that affect both the properties of epitaxial layers and the process formation of the composition of solid solutions in the sublattice of the fifth group.

Optimization of work on the selection of growing conditions for layers of solid substitution solutions in the fifth group with a given composition and properties is one of the tasks of developing a methodological base for the technology of growing heterostructures by the MBE method. The determination of the V group molecules fluxes values, that provide the required composition of solid solutions under the selected growth conditions, is carried out empirically. For this purpose, test samples are grown, their composition is determined and, if necessary, correction of the values of molecular fluxes is carried out. This approach is quite accurate and reliable, but time-consuming and expensive. Therefore, it is necessary to be able to perform an a priori assessment of the composition of the solid solution in the sublattice of the fifth group, depending on the growth conditions. Such a technique can be created on the basis of models that suggest the balance of mass transfer processes, provided that the stoichiometry of the compound is preserved.

The process of MBE of $A^{III}B^{V}$ materials is carried out under nonequilibrium conditions, nevertheless, the construction of such models is possible using both kinetic [5–15] and thermodynamic [16–21] approaches. We would like to note that these methods of theoretical consideration of growth processes are not competing. Their selection is determined by the goals and objectives of the researches. The areas of applicability of the thermodynamic approach based on the equations of acting masses in combination with the conservation of the mass of interacting elements are discussed in the review paper [19]. The attractiveness of the kinetic approach is due to the possibility of conducting theoretical studies at the level of elementary mass transfer processes occurring at the growth surfaces [12]. Kinetic models in combination with experimental data make it possible to analyze the adequacy of assumptions about the mechanisms of surface processes in MLE. The reliability of such an analysis, as well as the applicability of kinetic analysis in order to obtain quantitative dependences, are largely determined by the volume and level of detail of the experimental data base. This is due to the need to determine a priori a number of parameters that can only be estimated approximately from the first principles. In this connection, relatively simple kinetic models involving a minimum number of parameters are in demand. They are based on the assumption that, with growth, a stationary correlation is established between the processes of mass transfer, the composition of the surface and the composition of the volume of the film. At the same time, no explicit assumptions are made about the mechanisms for establishing stationary values of compositions [11].

Unfortunately, it is difficult to explain consistently the completeness of the experimental data presented in the literature within the framework of any one of the available simple kinetic models [15]. In [15], we proposed a kinetic model describing the process of formation of the composition of a solid solution $A^{III}P_xAs_{1-x}(001)$ in the sublattice of the fifth group at MBE from streams of As_2 and P_2 molecules on substrates with an α value less than 0.1°. It is based on the analysis of experimental data on the effect of epitaxy conditions on the proportion of phosphorus in GaP_xAs_{1-x}, AlP_xAs_{1-x} and InP_xAs_{1-x} relaxed films and includes consideration of replacement processes in the anionic layer on the surface of terraces outside the growth areas. The model adequately describes the dependence of x on the density of molecular fluxes, the substrate temperature and the stoichiometry of the surface, but it does not take into account the influence of the α value on the composition in the anionic sublattice of the solid solution. This article presents a model in which this limitation is eliminated.

2. EXPERIMENTAL DATA

In constructing the model, both experimental data [15] and newly obtained data on the effect of the angle of deviation of the substrate from the singular face (001) in the direction [110] on the proportion of phosphorus in GaP_xAs_{1-x} films were used. All samples were grown from As_2 and P_2 molecules on the "Shtat" MBE system, equipped with aperture crucible sources for Ga and arsenic and phosphorus dual-zone valve sources. The substrate temperature was monitored according to the indications of the control thermocouple of the substrate heater. The thermocouple was calibrated for each sample according to the surface superstructures (SS) transitions temperatures on GaAs(001) in the absence of an arsenic flux [22]. The flux densities of As_2 (J_{As_2}) and P_2 (J_{P_2}) molecules were determined by the values of the ion current of an ionization gauge converter introduced into direct fluxes of substances during measurements at the substrate position [23]. The average relative deviation from the original value of the fluxes for both elements was $\delta_J \approx \pm 5.5\%$. The density of the fluxes of Ga atoms (J_{Ga}) was determined by the reflection high-energy electron diffraction intensity oscillations. In the work [15] samples with films of

GaP_xAs_{1-x} solid solutions were grown on GaAs(001) offcut towards (111) by an angle α less than 0.1°. The parameters of the growth conditions varied in the following ranges: T_s from 400 to 600 °C; V_g from 0.25 to 2.5 μm/h; ratio $2J_{As_2}/J_{Ga}$ from 0.5 to 10; $2J_{P_2}/J_{Ga}$ ratio from 1 to 16. Sample thickness composition was 0.5–1 microns. It should be noted that GaP_xAs_{1-x} is not consistent in lattice constant with GaAs. The higher the value of x, the greater the discrepancy. When the growing GaP_xAs_{1-x} film reaches a critical thickness, the process of its plastic relaxation begins. In [15], all films of solid solutions had a thickness exceeding the critical value, which caused their relaxation in the range from 3 to 80%, depending on the composition and thickness. The films with a mismatch with GaAs of less than 0.65% had a low degree of relaxation.

In this work, epitaxial films GaP_xAs_{1-x} with a thickness of 1 μm were grown in one process on six GaAs substrates tilted away from the face (100) in the direction [110] by an angle $\alpha = 0.1°, 1°, 2°, 3°, 5°, 7°$ at $V_g = 1$ML/s (monolayer per second) and $T_s = 500$°C. The samples were examined by X- ray diffraction analysis, which made it possible to determine the average composition of the solid solution by the thickness of the film.

3. DESCRIPTION OF THE MODEL

The model is based on the following ideas about the MBE process of $A^{III}B^{V}$ compounds on the (001) substrates. The surface of the epitaxial layer is reconstructed. SS is formed by chemisorbed dimers of the fifth group elements (DV). Each SS corresponds to the degree of θ coverage with DV dimers. The superstructure of the surface may contain defects in the form of vacancies. The regions of existence and the state of each SS (composition + defectiveness) during growth are functions of *Ts*, the magnitude and ratio of the fluxes of the fifth group molecules (MV) and atoms of the third group. Each SS is stored in certain ranges of epitaxy conditions, which are easily controlled by the method of reflection high-energy electron diffraction. MV molecules and Ga atoms, colliding with the surface, pass into a physosorbed state. In this state, they move on the surface. The interaction of molecules and atoms with each other in the physosorbed layer is not considered. Elastic scattering of particles upon collision with a surface is not taken into account. Ga atoms from the physosorbed layer pass into the chemosorbed state only at the step kinks, forming sites for the chemisorption of V group molecules. MV molecules from the physosorbed state can either be desorbed or chemisorbed as dimers (MV → DV transition). Dimers DV under the action of thermal vibrations of the lattice are capable of leaving chemisorbed positions in the form of diatomic molecules. In general, these transitions will be denoted as DV → MV, and in particular DAs → As_2 and DP → P_2. During the DV → MV transition, vacancies are formed in the surface superstructure, which can be occupied as a result of chemisorption of both As_2 and P_2 molecules (As_2 → DAs and P2 → DP transitions, respectively).

In this model, it is assumed that the molecules formed during the DV → MV transition are desorbed without intermediate localization in the physosorbed state.

The vicinal surface (001) is terraced. In the model approximation, the width w of all terraces it is the same and is related to the value of α by the expression

$$w = \frac{a_{ss}}{2\mathrm{tg}\alpha}, \tag{1}$$

where a_{ss} is the lattice constant of the solid solution. There are kink on the steps bordering the terraces (Fig. 1). To simplify the image, the fractures are shown only with orientation $[\bar{1}10]$, but this does not affect the generality of further reasoning. The mechanism of kink formation and the statistics of their distribution along the edges of the terraces are not considered in the model. It will be shown below that only their presence is important. The growth process is represented as the incorporation of atoms of the third and fifth groups into the crystal lattice in the growth regions, localized in the step kinks. The anionic sublattice is filled with both As and P atoms, which are part of the SS in the form of dimers, and atoms from As_2 and P_2 molecules, which are chemisorbed directly in the growth region. As a result of chemisorption of Ga atoms, As_2 and P_2 molecules, a new reconstructed section of the terrace surface is formed in the growth region, shifting the kink along the step. The successive movement of the kinks causes the displacement of the edges of the terraces in the direction [110] (see Fig. 1). In one pass of the growth regions, the edge of the terrace discretely moves in the direction [110] for the width of the kink B. The width of the kink is assumed to be equal to the size of the SS unit cell in the direction [110].

The time of formation of one monolayer (τ_m) is inversely proportional to J_{Ga}:

$$\tau_m = \frac{2}{a_{ss}^2 J_{Ga}}. \tag{2}$$

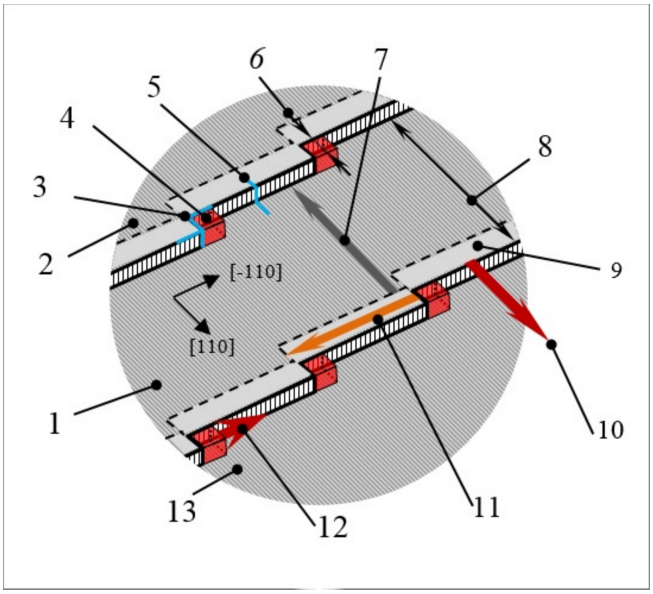

Fig. 1. Schema of the vicinal growth surface: 1 the terrace surface; 2 the surface of the upper terrace ; 3 the kink of step ; 4 the growth region; 5 the step; 6 the width of the kink B; 7 the x_a gradient (fractions of phosphorus atoms in SS) on the terrace surfaces; 8 the terrace width w; 9 the influence area of the terrace edge; 10 the terraces growth direction; 11 the x_a gradient along the steps; 12 the movement direction of growth regions; 13 the surface of the lower terrace

From the logic of the two-dimensional layered growth mechanism it follows that during the time of τ_m the edge of the terrace lying above is shifted by a distance equal to the width of the terrace lying below. In this case, the period of the motion of the growth regions (the time of updating the edge of the territory) is described by the expression

$$\tau = \frac{B\tau_m}{w}. \quad (3)$$

Thus, the time of updating the edge of the terrace τ is a function of τ_m and the angle of misorientation of the substrate surface and does not depend on the density and nature of the kink distribution along the steps. This conclusion suggested that the processes at the edges of the terraces may be responsible for the effect of α on the proportion of phosphorus x.

It is taken into account that during the transition from terrace to terrace, the translational symmetry of the SS is disrupted. This leads to the fact that the free energy of the edge elementary cells of the SS differs from the free energy of the cells removed from the edge of the terrace, which causes a difference in the values of the activation energy of the MV→DV transitions and the processes of dimer transition to the molecular state at the edge of the terrace and its surface. In the kinks, is not just a breakdown of translational symmetry. The structure of the layers of the lower terrace is changing locally in it. This creates conditions for a more effective interaction of atoms and molecules of the physosorbed layer with the centers of chemosorption in comparison with the edge and surface of the terraces. Here and further, the edge of the terrace is understood as a strip of surface oriented along the step, which is affected by the edge effects. It is assumed that the width of the edge of the terrace is equal to the width of the kink B. The replacement processes on the terraces surface and their edges occur as a result of the transition DV from SS in the molecular state and chemisorption of molecules in the resulting vacancies change the composition of SS formed in the growth area. This has an effect on the final value of x.

Based on the above provisions, the formation of the composition of a solid solution in an anion sublattice can be described by the following sequence of events.

I. At time t_s, a defect-free SS of a new terrace section is formed in the growth region. The composition of SS is determined by the growth parameters and the constants of the chemisorption processes of the fifth group molecules in the growth regions.

II. The change SS composition begin as a result of exchange adsorptiondesorption processes, which occur under conditions of the terrace edge effect from the SS formation moment and until the arrival of the next growth region at time t_e. The considered area of the surface is isolated from the influence of the terrace edge effect and becomes part of its surface after passing the growth zone. The change in SS as a result of exchange adsorption-desorption processes on the surface of the terrace lasts from the moment t_e until the moment t_f of the arrival of the growth region of the terrace lying above. At each moment of time, there is a gradient of SS composition repeating from kink to kink on the terrace edges, and on the surface of the terraces from their edges to the base of the terrace lying above (see Fig. 1). In the process of changing the composition, vacancy defects also accumulate in the SS.

III. At the moment of time t_f, the empty anion positions caused by the structure of the SS (recall that $\theta < 1$) and the formed vacancy defects are filled in the growth region. These

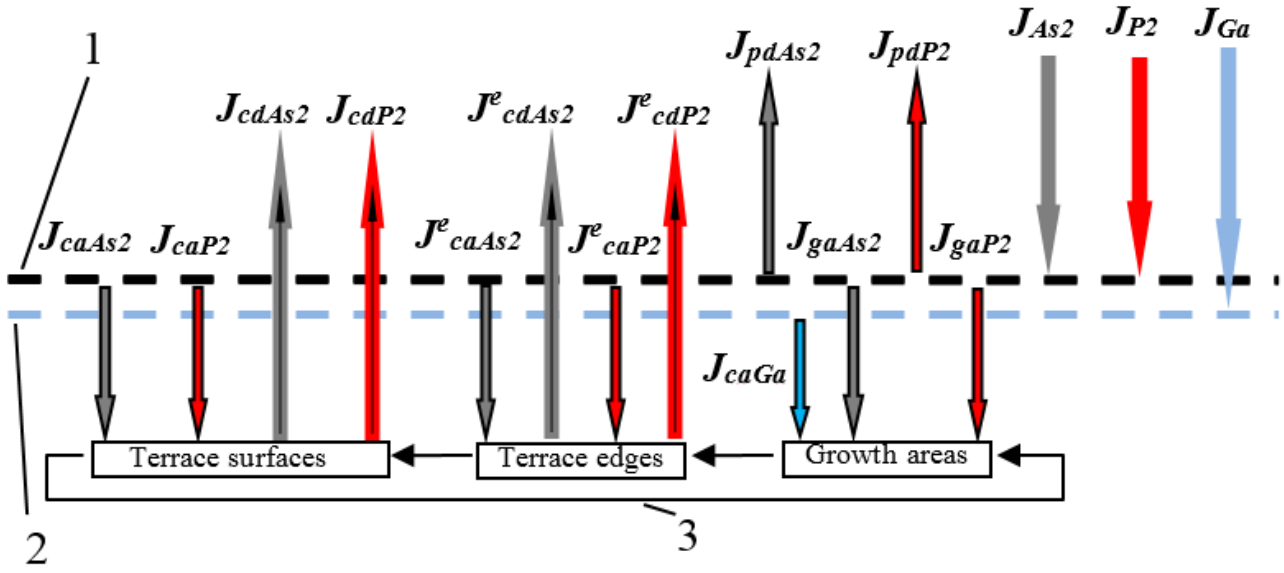

Fig. 2. Diagram of mass transfer processes on the growth surface: 1 layer of physosorbed As_2 and P_2 molecules; 2 layer of physosorbed Ga atoms; 3 sequence of changes in the composition of the SS

processes are accompanied by the process of filling the cation positions with gallium atoms. It is the formation of the cation layer in the growth region that fixes the composition of the solid solution in the sublattice of the fifth group. Stage (III) is inseparably followed by stage (I): the SS of the next section of the terrace surface lying above is formed on the cation sublayer. The scheme of mass transfer processes on the growth surface is shown in Fig. 2.

Table 1 shows the names of the processes indicated in Fig. 2 by arrows, and the corresponding formulas. The superscript *"e"* in the process symbols means that the processes take place on the terrace edge.

In Table 1, the following designations are used: n_{As_2} and n_{P_2}, concentrations of arsenic and phosphorus molecules in the physosorbed layer; n_{cAs} and n_{cP}, concentrations of arsenic and phosphorus dimers in the composition of SS on the surface of terraces; n^e_{cAs} and n^e_{cP} the concentration of arsenic and phosphorus dimers in the composition SS at the edges of terraces; v is the concentration of the chemosorption centers caused by DV → MV transitions; v_g is the concentration of chemisorption centers caused by the arrival of Ga atoms on the surface; n_0 the dimer concentration at $\theta = 1$; A is the parameter with dimension c^{-1}; E the process activation energy; R the universal gas constant. Note that the discussed model does not take into account the influence of elastic stresses in epitaxial films on the kinetics of the processes under consideration. Otherwise, it would be necessary to introduce assumptions about the laws linking, for example, parameters A and E with elastic stresses, which at this stage of the model development seems excessive.

In the growth region, the processes are fast and complete. Their duration can be neglected. The duration of the change in the SS composition outside the growth regions is determined by V_g. Theoretically, depending on V_g and T_s, the time to establish the steady state of the SS can be either less or more than τ_m. In the latter case, the duration of these processes should be taken into account, as it will affect the composition of x. All processes are interconnected through a layer of physosorbed As_2 and P_2 molecules. The spatial separation of the processes determines the heterogeneity of the molecules concentrations distribution in the physosorbed layer.

During the simulation, the real layer of the physosorbed molecules As_2 and P_2 was replaced by an equally distributed equivalent layer on the following bases. As_2 and P_2 molecules have high lateral mobility, which is due to the shallow depth of potential pits and, as a result, low diffusion activation energy. The diffusion lengths of the molecules reach several mcm [24]. All this causes smoothing of possible fluctuations in the concentrations of As_2 and P_2 molecules on the surface.

The model is implemented using a simulation approach. Mass transfer processes involving As_2, P_2 molecules and dimers DAs and DP were simulated, taking into account the

Table 1. Processes on the growth surface and their characteristics

No.	Process name	Formula	Process rate constant
1	Desorption of physosorbed molecules P_2	$J_{pd\mathrm{P}_2} = n_{\mathrm{P}_2} k_{pd\mathrm{P}_2}$	$k_{pd\mathrm{P}_2} = A_{pd\mathrm{P}_2} \exp\left(\frac{-E_{pd\mathrm{P}_2}}{RT_s}\right)$
2	Desorption of physosorbed molecules As_2	$J_{pd\mathrm{As}_2} = n_{\mathrm{As}_2} k_{pd\mathrm{As}_2}$	$k_{pd\mathrm{As}_2} = A_{pd\mathrm{As}_2} \exp\left(\frac{-E_{pd\mathrm{As}_2}}{RT_s}\right)$
3	Transition of phosphorus dimers to a molecular state with desorption into vacuum, DP→P_2 (terrace surface)	$J_{cd\mathrm{P}} = n_{c\mathrm{P}} k_{cd\mathrm{P}}$	$k_{cd\mathrm{P}} = A_{cd\mathrm{P}} \exp\left(\frac{-E_{cd\mathrm{P}}}{RT_s}\right)$
4	Transition of arsenic dimers to a molecular state with desorption into vacuum, DAs→As_2 (terrace surface)	$J_{cd\mathrm{As}} = n_{c\mathrm{As}} k_{cd\mathrm{As}}$	$k_{cd\mathrm{As}} = A_{cd\mathrm{As}} \exp\left(\frac{-E_{cd\mathrm{As}}}{RT_s}\right)$
5	DP→P_2 with vacuum desorption (terrace edge)	$J^e_{cd\mathrm{P}} = n^e_{c\mathrm{P}} k^e_{cd\mathrm{P}}$	$k^e_{cd\mathrm{P}} = A^e_{cd\mathrm{P}} \exp\left(\frac{-E^e_{cd\mathrm{P}}}{RT_s}\right)$
6	DAs→As_2 with desorption in the vacuum (terrace edge)	$J^e_{cd\mathrm{As}} = n^e_{c\mathrm{As}} k^e_{cd\mathrm{As}}$	$k^e_{cd\mathrm{As}} = A^e_{cd\mathrm{As}} \exp\left(\frac{-E^e_{cd\mathrm{As}}}{RT_s}\right)$
7	Chemisorption of P_2 → DP molecules (terrace surface)	$J_{ca\mathrm{P}_2} = n_{\mathrm{P}_2} \frac{\nu}{n_0} k_{ca\mathrm{P}_2}$	$k_{ca\mathrm{P}_2} = A_{ca\mathrm{P}_2} \exp\left(\frac{-E_{ca\mathrm{P}_2}}{RT_s}\right)$
8	Chemisorption of molecules As_2 → DAs (terrace surface)	$J_{ca\mathrm{As}_2} = n_{\mathrm{As}_2} \frac{\nu}{n_0} k_{ca\mathrm{As}_2}$	$k_{ca\mathrm{As}_2} = A_{ca\mathrm{As}_2} \exp\left(\frac{-E_{ca\mathrm{As}_2}}{RT_s}\right)$
9	P_2 →DP (terrace edge)	$J^e_{ca\mathrm{P}_2} = n_{\mathrm{P}_2} \frac{\nu_e}{n_0} k^e_{ca\mathrm{P}_2}$	$k^e_{ca\mathrm{P}_2} = A^e_{ca\mathrm{P}_2} \exp\left(\frac{-E^e_{ca\mathrm{P}_2}}{RT_s}\right)$
10	As_2 →DAs (terrace edge)	$J^e_{ca\mathrm{As}_2} = n_{\mathrm{As}_2} \frac{\nu_e}{n_0} k^e_{ca\mathrm{As}_2}$	$k^e_{ca\mathrm{As}_2} = A^e_{ca\mathrm{As}_2} \exp\left(\frac{-E^e_{ca\mathrm{As}_2}}{RT_s}\right)$
11	Chemisorption of P_2 molecules in the growth area	$J_{ga\mathrm{P}_2} = n_{\mathrm{P}_2} \frac{\nu_g}{n_0} k_{ga\mathrm{P}_2}$	$k_{ga\mathrm{P}_2} = A_{ga\mathrm{P}_2} \exp\left(\frac{-E_{ga\mathrm{P}_2}}{RT_s}\right)$
12	Chemisorption of As_2 molecules in the growth region	$J_{ga\mathrm{As}_2} = n_{\mathrm{As}_2} \frac{\nu_g}{n_0} k_{ga\mathrm{As}_2}$	$k_{ga\mathrm{As}_2} = A_{ga\mathrm{As}_2} \exp\left(\frac{-E_{ga\mathrm{As}_2}}{RT_s}\right)$

localization of these processes and in relation to the state of the surface, as well as with the preservation of the logical structure and sequence of their course in time and space. The algorithm for calculating the proportion of phosphorus in a solid solution is divided into two stages: 1) calculation of the concentration values of n_{As_2} and n_{P_2}; 2) with known n_{As_2} and n_{P_2}, for each stage of formation of the composition of the solid solution (I, II and III), the values of other model dependent variables necessary for calculating the proportion of phosphorus are sequentially calculated. The x fraction is formed in the growth region both from atoms, already included in the composition of SS in the form of DV dimers, as well as from atoms of n_{As_2} and n_{P_2} molecules, chemosorbable on empty anionic positions:

$$x = \frac{\left(n_0 - n_{f\mathrm{P}} - n_{f\mathrm{As}}\right)x_{a_0} + n_{f\mathrm{P}}}{n_0}, \qquad (4)$$

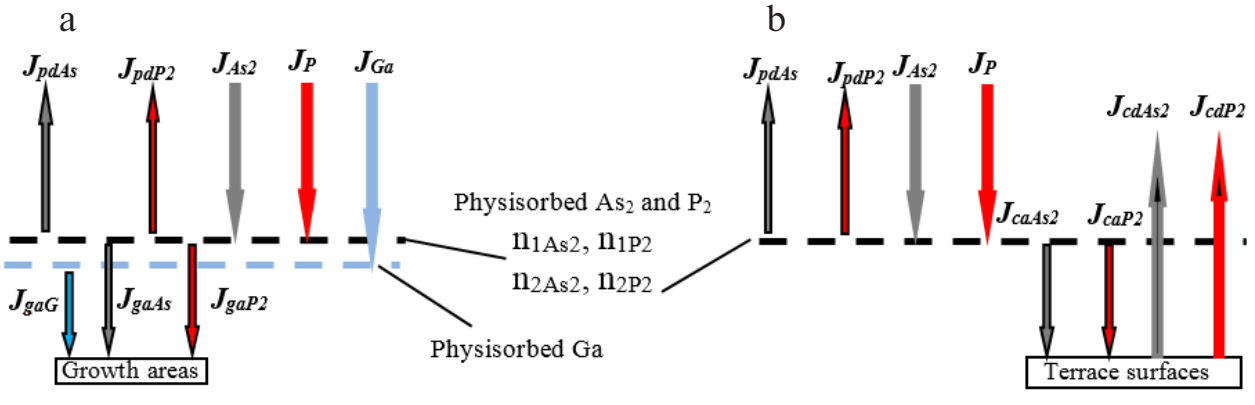

Fig. 3. Diagrams of mass transfer processes for calculating n_{As_2} and n_{P_2}. a scheme S1, b scheme S2

where x_{a_0} is the proportion of phosphorus atoms embedded in anionic positions in the growth region; $n_{f\mathrm{As}}$ and $n_{f\mathrm{P}}$ are the concentrations of arsenic and phosphorus dimers remaining in the SS by the time of the arrival of the terrace growth area of the terrace located above. The difference between $n_0 - n_{f\mathrm{P}} - n_{f\mathrm{As}}$ gives the total concentration of vacancy defects in SS and free anion positions due to the structure of SS. Both vacancies and structurally determined empty anionic positions are filled at stage III with As and P atoms in proportions determined by the corresponding chemisorption constants and concentrations of n_{As_2} and n_{P_2}. The proportion of phosphorus in the SS, which is formed at stage I, equal to x_{a_0}. The values of $n_{f\mathrm{As}}$ and $n_{f\mathrm{P}}$ are found from solving systems of equations (5) and (6):

$$\begin{aligned}\frac{\theta n_0 - n^e_{c\mathrm{P}} - n^e_{c\mathrm{As}}}{n_0} n_{P_2} k^e_{caP} \partial t - n^e_{c\mathrm{P}} k^e_{cd\mathrm{P}} \partial t = \partial n^e_{c\mathrm{P}},\\ \frac{\theta n_0 - n^e_{c\mathrm{As}} - n^e_{c\mathrm{As}}}{n_0} n_{As_2} k^e_{ca\mathrm{As}} \partial t - n^e_{c\mathrm{As}} k^e_{cd\mathrm{As}} \partial t = \partial n^e_{c\mathrm{As}},\end{aligned} \tag{5}$$

where $n^e_{c\mathrm{P}}$ and $n^e_{c\mathrm{As}}$ are concentrations of arsenic and phosphorus dimers on the formed surface area at the current time from the range from t_s to t_e. The $n^e_{c\mathrm{As}}$ value varies from $n_{sAs} = \mathrm{n}_0\theta(1 - x_{a_0})$ to $n^e_{f\mathrm{As}}$, and $n^e_{c\mathrm{P}}$ from $n_{sP} = \mathrm{n}_0\theta x_{a_0}$ to $n^e_{f\mathrm{P}}$. The values of $n^e_{f\mathrm{As}}$ and $n^e_{f\mathrm{P}}$ serve as the initial conditions for the system

$$\begin{aligned}\frac{\theta n_0 - n_{c\mathrm{P}} - n_{c\mathrm{As}}}{n_0} n_{P_2} k_{caP_2} \partial t - n_{c\mathrm{P}} k_{cd\mathrm{P}} \partial t = \partial n_{c\mathrm{P}},\\ \frac{\theta n_0 - n_{c\mathrm{P}} - n_{c\mathrm{As}}}{n_0} n_{As_2} k_{ca\mathrm{As}_2} \partial t - n_{c\mathrm{As}} k_{cd\mathrm{As}} \partial t = \partial n_{c\mathrm{As}},\end{aligned} \tag{6}$$

where $n_{c\mathrm{P}}$ and $n_{c\mathrm{As}}$ are the concentrations of arsenic and phosphorus dimers on the formed surface area at the current time from the range from t_e to t_f. At the same time, $n_{c\mathrm{As}}$ changes from $n^e_{f\mathrm{As}}$ to $n_{f\mathrm{As}}$, and $n_{c\mathrm{P}}$ from $n^e_{f\mathrm{P}}$ to $n_{f\mathrm{P}}$.

The values of n_{As_2} and n_{P_2} are found numerically by simulating the establishment of stationary concentrations in the approximation of unlimited mobility of As_2 and P_2 molecules. All mass transfer processes affecting n_{As_2} and n_{P_2} are taken into account, except for processes at the edges of terraces, which have a negligible effect on the concentration of molecules in the physosorbed state. The presence of an SS gradient on the surface of the terraces is also taken into account.

The considered mass transfer processes are combined into two groups. The first group includes the processes occurring only in the growth areas of the S1 mass transfer scheme (Fig. 3*a*). The second one is only about processes on the surface of terraces outside the growth areas scheme S2 (Fig. 3*b*). The task is solved in parts. The effect of the process groups S1 and S2 on the concentrations of n_{As_2} and n_{P_2} separately is considered (approximation of complete isolation). Further, the obtained partial values of n_{1As_2} and n_{1P_2} concentrations for the case of S1 and n_{2As_2} and n_{2P_2} for S2 are used to estimate the values of n_{As_2} and n_{P_2} concentrations in the quasi- isolated coexistence of schemes S1 and S2 during their interaction through the physosorbate layer.

Let's consider the S1 scheme in the approximation of complete isolation. Formation of the anionic composition of the surface (the formation of the phosphorus fraction x_{a_0}) is realized due to the chemisorption of As_2 and P_2 molecules on metals formed due to the chemisorption of gallium atoms. The anionic composition of the solid solution surface and volume are identical, i.e. $x_{a_0} = x$, where $x_a = n_{c\mathrm{P}}/(n_{c\mathrm{As}} + n_{c\mathrm{P}}) = n_{c\mathrm{P}}/\mathrm{n}_0$. Taking into account the listed conditions, it is possible to write a system of equations linking the balance of mass transfer processes and solid solution composition:

$$\begin{aligned} J_{\mathrm{P}_2} &= J_{pd\mathrm{P}_2} + J_{ca\mathrm{P}_2}, \\ J_{\mathrm{As}_2} &= J_{pd\mathrm{As}_2} + J_{ca\mathrm{As}_2}, \\ xJ_{\mathrm{Ga}} &= 2J_{ca\mathrm{P}_2}, \\ (1-x)J_{\mathrm{Ga}} &= 2J_{ca\mathrm{As}_2}. \end{aligned} \tag{7}$$

Taking into account the expressions from Table 1 (see lines 1, 2, 11, 12), the system (7) is reduced to the equation

$$\frac{J_{\mathrm{As}_2} / (1-x) - 0.5J_{\mathrm{Ga}}}{J_{\mathrm{P}_2} / x - 0.5J_{\mathrm{Ga}}} \frac{k_{pd\mathrm{P}_2}}{k_{pd\mathrm{As}_2}} \frac{k_{ca\mathrm{As}_2}}{k_{ca\mathrm{P}_2}} = 1. \tag{8}$$

The solution of equation (8) with respect to $x = x_{a_0}$ gives the proportion of phosphorus in the solid solution GaP_xAs_{1-x}. Knowing x_{a_0}, it is possible to calculate the concentrations of As_2 and P_2 molecules in the physosorbed layer to approximate S1 $n_{1\mathrm{As}_2}$ and $n_{1\mathrm{P}_2}$:

$$\begin{aligned} n_{1\mathrm{P}_2} &= \frac{J_{\mathrm{P}_2} - 0.5J_{\mathrm{Ga}}x}{k_{pd\mathrm{P}_2}}, \\ n_{1\mathrm{As}_2} &= \frac{J_{\mathrm{As}_2} - 0.5J_{\mathrm{Ga}}x}{k_{pd\mathrm{As}_2}}. \end{aligned} \tag{9}$$

Now let's consider the S2 scheme in the approximation of complete isolation. When the growth area passes, a reconstructed layer of arsenic and phosphorus is formed on the surface of the terrace. The composition of this layer changes further as a result of transitions DV → MV and MV → DV until the arrival of the next growth region of the top terrace. The total time of change in the composition of the SS is equal to the time of growth of one monolayer. A local change in composition can be represented as a sequence of changes in the SS state. We assume that a sequence from C phases of the SS state is simultaneously present on the surface. Each phase contributes to the formation of the concentration of As_2 and P_2 molecules in the physosorbed state. The task is to determine and average these contributions. The state of each i-th phase differs slightly from the $(i\pm1)$-th phase. The phases from $i = 1$ to $i = C$ cover the entire range of changes in the state of the SS from the moment t_0 formation of the initial composition in the growth region up to the time $t = t_0 + \tau_m$. The proportion of each phase in the composition of the surface is equal to C^{-1}. Moreover, the regions i are isolated from each other. In this approximation, the concentrations of As_2 and P_2 molecules for each of the i-th domain, as well as $n_{c\mathrm{As}}$ and $n_{c\mathrm{P}}$, can be found from solving a system of equations

$$\begin{aligned} &J_{\mathrm{P}_2}\partial t - n_{2\mathrm{P}_2 i}k_{pd\mathrm{P}_2}\partial t - \\ &- \frac{\theta n_0 - n_{c\mathrm{P}_i} - n_{c\mathrm{As}_i}}{n_0} n_{2\mathrm{P}_2 i}k_{ca\mathrm{P}_2}\partial t = \partial n_{2\mathrm{P}_2 i}, \\ &J_{\mathrm{As}_2}\partial t - n_{2\mathrm{As}_2 i}k_{pd\mathrm{As}_2}\partial t - \\ &- \frac{\theta n_0 - n_{c\mathrm{P}_i} - n_{c\mathrm{As}_i}}{n_0} n_{2\mathrm{As}_2 i}k_{ca\mathrm{As}_2}\partial t = \partial n_{2\mathrm{As}_2 i}, \\ &- n_{c\mathrm{P}_i}k_{cd\mathrm{P}}\partial t + \frac{\theta n_0 - n_{c\mathrm{P}_i} - n_{c\mathrm{As}_i}}{n_0} \times \\ &\times n_{2\mathrm{P}_2 i}k_{ca\mathrm{P}_2}\partial t = \partial n_{c\mathrm{P}_i}, \\ &- n_{c\mathrm{As}_i}k_{cd\mathrm{As}}\partial t + \frac{\theta n_0 - n_{c\mathrm{P}_i} - n_{c\mathrm{As}_i}}{n_0} \times \\ &\times n_{2\mathrm{As}_2 i}k_{ca\mathrm{As}_2}\partial t = \partial n_{c\mathrm{As}_i}. \end{aligned} \tag{10}$$

The solution of the system (10) was found by numerical methods. The initial values of the concentrations of molecules As_2 and P_2 in the physosorbed state, $n_{2\mathrm{As}_2}$ and $n_{2\mathrm{P}_2}$, and the initial values of the concentrations of $n_{c\mathrm{P}}$ and $n_{c\mathrm{As}}$ are calculated according to the S1 scheme. The solution of the system for the i-th phase is sought for a time interval equal to $\tau_m C^{-1}$.

Average values of molecular concentrations arsenic and phosphorus in the physosorbed layer are calculated as the arithmetic mean:

$$\begin{aligned} n_{2\mathrm{P}_2} &= \sum_{i=1}^{C} \frac{n_{2\mathrm{P}_2 i}}{C}, \\ n_{2\mathrm{As}_2} &= \sum_{i=1}^{C} \frac{n_{2\mathrm{As}_2 i}}{C}. \end{aligned} \tag{11}$$

The concentrations of n_{As_2} and n_{P_2} under the conditions of interaction of quasi-isolated modes S1 and S2 through a layer of physosorbed molecules As_2 and P_2 are calculated as follows. Partial equivalent balance systems of equations for S1 and S2 are compiled, as well as the equivalent system of equations for the joint implementation of modes S1 and S2.

The system of equations for the S1 scheme:

$$\begin{aligned} J_{\mathrm{As}_2} &= n_{1\mathrm{As}_2}k_{pd\mathrm{As}_2} + n_{1\mathrm{As}_2}K_{ga\mathrm{As}_2}, \\ J_{\mathrm{P}_2} &= n_{1\mathrm{P}_2}k_{pd\mathrm{P}_2} + n_{1\mathrm{P}_2}K_{ga\mathrm{P}_2}, \end{aligned} \tag{12}$$

where $K_{ga\mathrm{As}_2}$ and $K_{ga\mathrm{P}_2}$ are equivalent chemosorption constants in the growth regions; $n_{1\mathrm{As}_2}$ and $n_{1\mathrm{P}_2}$ average-concentrations of As and P molecules found according to the S1 scheme.

The system of equations for the S2 scheme:

$$\begin{aligned} J_{As_2} &= n_{2As_2} k_{pdAs_2} + n_{2As_2} K_{caAs_2}, \\ J_{P_2} &= n_{2P_2} k_{pdP_2} + n_{2P_2} K_{caP_2}, \end{aligned} \tag{13}$$

where K_{caAs_2} and K_{caP_2} are equivalent chemisorption constants on the terrace surface; n_{2As_2} and n_{2P_2} are the average concentrations of arsenic and phosphorus molecules found in the S2 approximation. The joint implementation of the S1 and S2 modes leads to a system of equations

$$\begin{aligned} J_{As_2} &= n_{As_2} k_{pdAs_2} + n_{As_2} K_{caAs_2} + n_{As_2} K_{gaAs_2}, \\ J_{P_2} &= n_{P_2} k_{pdP_2} + n_{P_2} K_{caP_2} + n_{P_2} K_{gaP_2}. \end{aligned} \tag{14}$$

The systems of equations (12) and (13) allow us to find an expression for K_{gaAs_2} and K_{gaP_2}, K_{caAs_2} and K_{caP_2}, which, after substitution into the system (14), will give a solution for n_{As_2} and n_{P_2}:

$$\begin{aligned} n_{As_2} &= \frac{J_{As_2} n_{1As_2} n_{2As_2}}{J_{As_2} n_{1As_2} + J_{As_2} n_{2As_2} - k_{pdAs_2} n_{1As_2} n_{2As_2}}, \\ n_{P_2} &= \frac{J_{P_2} n_{1P_2} n_{2P_2}}{J_{P_2} n_{1P_2} + J_{P_2} n_{2P_2} - k_{pdP_2} n_{1P_2} n_{2P_2}}. \end{aligned} \tag{15}$$

4. NUMERICAL IMPLEMENTATION OF THE MODEL

4.1. Criteria for evaluating the reliability of models

The quantitative criterion for evaluating the reliability of the model in describing the temperature dependence of the phosphorus fraction x was the value of δ_T:

$$\delta_T = \frac{1}{h} \sum_{j=1}^{h} \left| \frac{x_{cj} - x_{ej}}{x_{ej}} \right|, \tag{16}$$

where h is the number of samples in the corresponding group. The assessment was carried out using data samples with a fixed T_s value = 400, 410, 500, 550, 580, 600 °C and a growth rate of approximately 1 ML/s. The value δ_V was chosen as a quantitative criterion for evaluating the reliability of the model when describing the dependence of the proportion of phosphorus x on the growth rate:

$$\delta_V = \frac{1}{k} \sum_{j=1}^{k} \left| \frac{x_{cj} - x_{ej}}{x_{ej}} \right|, \tag{17}$$

where k is the number of samples in the group. Groups with V_g = 0.25, 0.49, 0.98, 1.01, 1.4, 2, 2.2 ML/s at a growth temperature T_s = 500–510 °C were considered.

The quantitative criterion for evaluating the reliability of the model in describing the dependence of the phosphorus fraction x on the deviation angle of the substrate was the value of δ_α:

$$\delta_\alpha = \frac{1}{m} \sum_{j=1}^{m} \left| \frac{x_{cj} - x_{ej}}{x_{ej}} \right|, \tag{18}$$

where m is the number of samples in the group.

4.2. Errors in the definition of J_{As_2} and J_{P_2}

Even if the mathematical model is completely reliable, the values of x_c will differ from x_e. This is due to a number of reasons, including the presence of errors in determining the values of molecular flux density and T_s. The influence of the error in determining J_{Ga} can be neglected, since the method of measuring the growth rate and the accuracy of maintaining flux densities give an error of no more than 1%. The technique for determining the flux density of As_2 and P_2 molecules is less accurate. There is also instability of the sources of the arsenic and phosphorus molecules. In this regard, an assessment was made of the possible deviation of x_c from x_e due to inaccuracies in the definition of J_{As_2}, J_{P_2} and T_s. For this purpose, the model values of the phosphorus fractions x_{c0}, x_{c1} and x_{c2} were calculated at nominal densities J_{0As_2}, J_{0P_2} and diagonally offset values $J_{maxAs_2} = J_{0As_2}$ (1+0.055) and $J_{minP_2} = J_{0P_2}$ (1–0.055), as well as $J_{minAs_2} = J_{0As_2}$ (1–0.055) and $J_{maxP_2} = J_{0P_2}$ (1+0.055), respectively. When calculating x_{c0}, the substrate temperature was assumed to be equal to T_{s0}. When calculating x_{c1} and x_{c2}, the absolute error modulus T_s (±2.5°) was added or subtracted from T_{s0} so that the differences $x_{c1} - x_{c0}$ and $x_{c2} - x_{c0}$ had the highest absolute value. Next, the values were calculated

$$\delta_{c1} = \frac{1}{l} \sum_{j=1}^{l} \left| \frac{x_{c1j} - x_{c0j}}{x_{c0j}} \right|, \tag{19}$$

$$\delta_{c2} = \frac{1}{l} \sum_{j=1}^{l} \left| \frac{x_{c2j} - x_{c0j}}{x_{c0j}} \right|, \tag{20}$$

where l is the number of pairs of values J_{0As_2} and J_{0P_2}. Values from an array of experimental data were used for J_{0As_2}, J_{0P_2} and Ts_0. The largest value of δ_{max} from the pair δ_{c1} and δ_{c2} was chosen as the largest possible relative deviation of the x_c from x_e.

4.3. Kinetic parameters of the model

The data available in the literature allow only an approximate estimation of the model kinetic parameters. Thus, in [25], the values of the activation energy of the desorption of As_4 and P_4 molecules from the adsorption layer are given. In the As_4 case, the activation energy of desorption is 46.30 kJ/mol, and in the case of P_4 30.80 kJ/mol. There are no reliable experimental data on the binding energy of As_2 and P_2 molecules with the surface of $A^{III}B^{V}(001)$ in the physosorbed state. The values obtained in [25] for As_4 and P_4 are taken as the initial value for As_2 and P_2 molecules desorption activation energy from the physisorbed state. The initial values of the activation energy of the transition of arsenic and phosphorus dimers to the molecular state were assumed to be 267 kJ/mol [26]. The differences in activation energies for the DAs→ As_2 and DP → P_2 transitions were determined during the selection of model parameter values. The activation energy of the chemisorption of molecules was estimated as a fraction of the activation energy of the transition to the molecular state. The share coefficient varied from 0.10 to 0.50. Multipliers A were selected from the range 10^{12}–10^{14} c^{-1}. It is accepted that the processes of chemisorption in the growth areas are of a non- activation nature. This approach is justified, since, for example, the GaAs MBE process is implemented at 200 °C and below. The chemisorption rate constants for the growth regions are the same for As_2 and P_2 molecules and in all cases equal to $6.0 \cdot 10^{12}$ c^{-1}.

4.4. Calculation results

Fig. 4 shows the results of calculating the proportion of phosphorus depending on α using the proposed model in comparison with experimental data. The model satisfactorily reflects the tendency of x to change with increasing α. In Table 2 data on the arithmetic mean values of the modules of relative deviations x_c from x_e for temperature, velocity and angular dependences are presented. The maximum deviations of δ_{max} are approximately 0.105.

The model allows us to obtain values of relative deviations less than δ_{max} consistent in temperature and growth rate for the entire array of experimental data from [15], as well as for newly obtained data on the influence of α. Table 3 shows the found values of the kinetic parameters of the model.

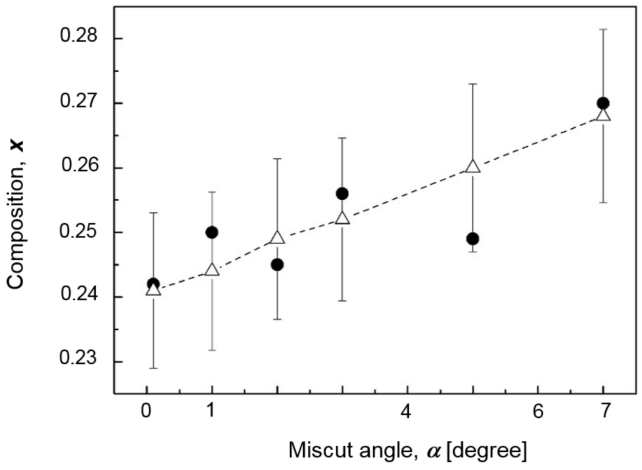

Fig. 4. Dependences of the proportion of phosphorus x in a solid solution GaP_xAs_{1-x} from the substrate misorientation angle from the face (001). Black circles are experimental data; white triangles are calculated values. The points corresponding to the model values of x are connected by lines in order to facilitate the perception of graphical information

Table 2. Arithmetic mean values of the modules of relative deviations of x_c from x_e

Dependence on T_s		Dependence on V_g		Dependence on α	
T_s, °C	δ_T	V_g, MC/c	δ_V	α	δ_α
400	0.039	0.25	0.023	0.1°	0.013
410	0.06	0.50	0.069	1°	0.029
450	0.061	0.98	0.063	2°	0.01
500	0.058	1.01	0.038	3°	0.018
550	0.014	1.38	0.015	5°	0.039
580	0.054	1.98	0.024	7.5°	0.014
600	0.039	2.20	0.085	7.5°	0.014

5. DISCUSSION OF THE RESULTS

Before proceeding to the discussion of the results, we recall that when constructing the model, non-stationary exchange processes occurring on the surfaces and edges of terraces are taken into account. The replacement processes change the anionic composition of the surface formed in the growth regions localized at the steps, edges. The duration of the change in the anionic composition on the terrace surface is determined by the time of formation of one monolayer, and at the terrace edges by the frequency of their renewal. The formation time of one monolayer is uniquely determined by the gallium atoms flux density, and the time of renewal of the terrace edges depends on both J_{Ga} and α. At the same

time, the pace of implementation elementary processes is controlled by the substrate temperature. According to the model, it is the correlation of the contributions of the listed factors that determines the features of the x dependence on the growth conditions. The data presented in Table 2 allow us to conclude that the model satisfactorily describes the dependence of x on J_{Ga}, J_{As_2}, J_{P_2}, T_s, V_g and α.

The introduction to consideration of nonstationary exchange processes at the edges of terraces outside the growth areas made it possible to take into account the influence of α on the formation of the anionic composition of the solid solution. The mechanism of influence of α is as follows. With increasing α, increases the density of the steps, which causes an increase in the renewal period of the terrace edge (see Fig. 1). The duration of the change in the composition of the SS at the edge of the terrace also increases due to the combined processes DV → MV and MV → DV, shifting the composition towards a greater proportion of phosphorus. Note that the spread of experimental data in Fig. 4 may be due to the deviation of the substrate surface misorientation azimuth from the direction [110]. On an ideal surface, this leads to the appearance of steps oriented both along [110] and along $[\bar{1}10]$. According to the work [27] The efficiency of embedding Ga atoms in the orientation stage [110] differs from the efficiency of embedding in the orientation stage $[\bar{1}10]$. An analogous effect is probably observed in the case of arsenic and phosphorus molecules, which may react differently to a change in the orientation of the edge of the terrace, which is the subject of a separate study.

Another manifestation of the presence of non- stationary processes in GaP_xAs_{1-x} MBE on the vicinal surface is the dependence of x on V_g as an independent factor [15]. The difficulty of detecting this effect experimentally is due to the fact that with a change in the density of the gallium flux, all other things being equal, both the total value of the V/III ratio in flows and its partial components change. The change in these relations causes a shift in the composition of the growing film, which is not caused by a change in the growth rate [15]. Thus, according to data [15], all other things being equal, an increase in both the integral ratio $(J_{As_2} + J_{P_2})/J_{Ga}$ and the partial ratios J_{As_2}/J_{Ga} and J_{P_2}/J_{Ga} leads to a decrease in the efficiency of phosphorus embedding relative to the efficiency of arsenic embedding. In Fig. 5 the experimental data from [15] are indicated by black circles, and the corresponding values calculated using the discussed model are indicated by white triangles. The experiment/model data pairs are numbered from 1 to 6. In the presented

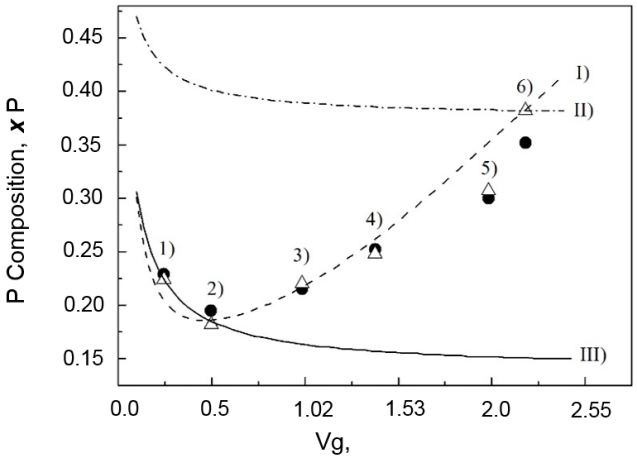

Fig. 5. Dependences of the phosphorus proportion x in the solid solution GaP_xAs_{1-x} on the growth rate at $T_s = 500$ °C for various values of the ratios $(J_{As_2} + J_{P_2})/J_{Ga}$ and $J_{P_2}/(J_{As_2} + J_{P_2})$ given in the text

data series, the growth rate varies discretely from 0.25 ML/s for 1 to 2.18 ML/s for 6, and the $J_{P_2}/(J_{As_2} + J_{P_2})$ ratio ranges from 0.62 to 0.69. In this case, the $(J_{As_2} + J_{P_2})/J_{Ga}$ ratio takes the following values: 20.63 for 1; 8.99 for 2; 5.08 for 3; 3.25 for 4; 2.29 for 5; 2.52 for 6.

Line I shows the model dependence of the phosphorus fraction on the growth rate at constant values of J_{As_2}, J_{P_2} and $J_{P_2}/(J_{As_2} + J_{P_2}) = 0.688$. For this dependence, with an increase in the growth rate from 0.24 ML/s to 2.35 ML/s, the ratio $(J_{As_2} + J_{P_2})/J_{Ga}$ varies from 22.49 to 2.25. The decrease in the x with a decrease in the growth rate to $V_g \simeq 0.5$ ML/s is due to the predominance of the effects of changing the ratio $(J_{As_2} + J_{P_2})/J_{Ga}$. Further, the influence of the growth rate begins to dominate. The most obvious effect of V_g on the formation of the solid solution composition is manifested when the conditions $(J_{As_2} + J_{P_2})/J_{Ga} = \text{const}$, $J_{P_2}/(J_{As_2} + J_{P_2}) = \text{const}$ and $T_s = \text{const}$ are met. When these requirements are fulfilled, the main contribution to the formation of the composition in the field of low growth rates is made by the duration of replacement processes DV → MV and MV → DV both on the surface and on the edges of terraces outside the growth regions. The smaller the V_g, the greater the τm and the longer the change in the composition of the SS takes. Model dependences for these conditions are represented by lines II and III in Fig. 5. Dependence II is constructed for the relations $J_{P_2}/(J_{As_2} + J_{P_2}) = 0.69$ and $(J_{As_2} + J_{P_2})/J_{Ga} = 2.52$, and III for $J_{P_2}/(J_{As_2} + J_{P_2}) = 0.681$ and

$(J_{As_2} + J_{P_2})/J_{Ga} = 20.63$. The shift of the composition in the area of large values of x with a decrease in V_g (lines II and III in Fig. 5) due to the fact that the rate constant of the DAs → As_2 process is significantly higher than the rate constant of the DP → P_2 process both on the surface and on the edges of the terraces.

The model describes the behavior of x depending on T_s in the entire studied temperature range from 400 to 600 °C, and the curve of change in the phosphorus proportion has a complex form [15]. Figure 6 shows the experimental data from [15] in circles, and the triangles are the calculated values obtained using the discussed model for the same growth conditions. The samples corresponding to the data pairs experiment/model 1–7 were grown at the following T_s values: 1 – 400 °C; 2 – 450 °C; 3 – 500 °C; 4 – 550 °C; 5 – 580 °C; 6 and 7 – 600 °C. The ratios of molecular fluxes $(J_{As_2} + J_{P_2})/J_{Ga}$ and $J_{P_2}/(J_{As_2} + J_{P_2})$ during sample growth had the following values, respectively: 1 – 6.04 and 0.73; 2 – 5.95 and 0.71; 3 – 5.08 and 0.69; 4 – 5.88 and 0.67; 5 – 4.29 and 0.57; 6 – 3.99 and 0.58; 7 – 5.16 and 0.7. The lines in Fig. 6 indicate the model dependences of the phosphorus fraction to the substrate temperature. Line I is plotted for the values $(J_{As_2} + J_{P_2})/J_{Ga}$ and $J_{P_2}/(J_{As_2} + J_{P_2})$ corresponding to the growth conditions of sample 7, and II to 5. A change in the ratio of $(J_{As_2} + J_{P_2})/J_{Ga}$ and $J_{P_2}/(J_{As_2} + J_{P_2})$ leads to a shift in the model dependence along the coordinate axes without significantly changing its appearance.

The observed shape of the curves is explained by the exponential dependence of the mass transfer processes rate constants occurring on the surface and terraces edges on T_s. The unsteadiness of these processes also makes a certain contribution. The higher the T_s, the higher the pace of the processes. In the range of relatively low T_s values, the contribution of replacement processes DV → MV and MV → DV on the surface and edges of terraces in the composition formation of the solid solution with increasing T_s will change slightly. With a further increase in T_s, the efficiency of replacement processes will increase. The activation energy of the DAs → As_2 transition is lower than the activation energy of the DP → P_2 transition. This explains the increase in the proportion of phosphorus with increasing temperature. With an increase in T_s, the difference between the desorption rate constants of phosphorus and arsenic dimers begins to decrease (due to the exponential nature of constants). Therefore, in the high temperature region, the effect of temperature on the solid solution composition decreases, which was observed in [15].

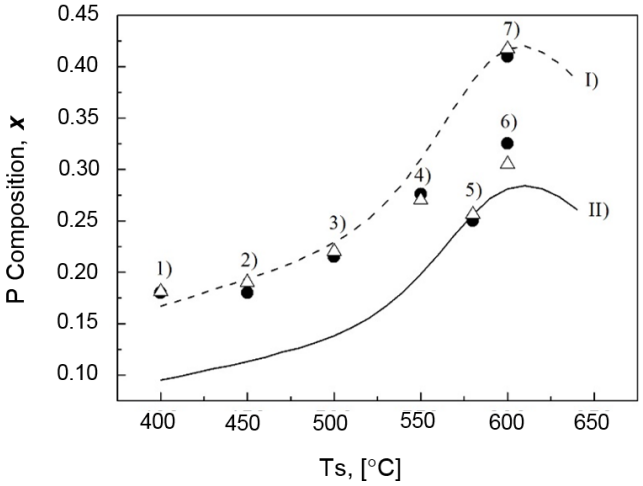

Fig. 6. The dependences of the phosphorus proportion x in the solid solution GaP_xAs_{1-x} on the temperature of the substrate T_s at a growth rate of 1 ML/s. The black circles represent the experimental data from [15], and the white triangles represent the calculated values. Lines indicate the calculated dependences of the phosphorus fraction on T_s. Dependencies differ in the values $(J_{As_2} + J_{P_2})/J_{Ga}$ and $J_{P_2}/(J_{As_2} + J_{P_2})$, see the text

It follows from the data in Table 3 that outside the growth regions of the activation energy of the As_2 → DAs transitions and P_2 → DP, varying depending on the location, remain equal to each other. On the terrace surfaces the activation energy is higher, and on the terrace edges lower. The activation energies of MV → DV transitions in the model are relatively small. Within the framework of the considered model approaches, such a level of activation energies is quite justified. Changing their values towards a noticeable increase makes it impossible to reconcile x_c with x_e at 500 °C and above. The equality of the activation energies of As_2 → DAs transitions and P_2 → DP is due to the following. The main source of energy for overcoming the thresholds of activation of diffusion, desorption and chemisorption of molecules As_2 and P_2 is the lattice thermal oscillation. The MV → DV transition is realized if the gallium atoms that are part of the vacancy complex are in an activated state. The energy level required for their activation may exceed the activation energy level of desorption of molecules from the physosorbed state, which is observed in the case of phosphorus. But desorption is not realized at the same time, since a significant part of energy is localized on gallium atoms chemically bonded to the surface, and the time required for the interaction of the molecule and excited gallium atoms is limited.

Table 3. Values of the parameters of the process rate constants

Process	Process speed constant		Parameter value	
	E	A	E, kJ/mol	A, $c^{-2}/10^{12}$
Desorption of molecules from a physosorbed state	E_{pdAs_2}	A_{pdAs_2}	43.94	6.37
	E_{pdP_2}	A_{pdP_2}	26.59	6.62
Chemisorption of molecules of the fifth group, MV → DV (surface)	E_{caAs_2}	A_{caAs_2}	34.24	0.20
	E_{caP_2}	A_{caP_2}	34.24	1.27
Chemisorption of molecules of the fifth group, MV → DV (edges of terraces)	E_{ecaAs_2}	A_{ecaAs_2}	31.33	5.75
	E_{ecaP_2}	A_{ecaP_2}	31.33	6.37
Transition of dimers of the fifth group to the molecular state, DV → MV (surface)	E_{cdAs}	A_{cdAs}	206.10	6.37
	E_{cdP}	A_{cdP}	223.10	5.47
Transition of dimers of the fifth group to the molecular state, DV → MV (edges of terraces)	E_{ecdAs}	A_{cdAs}	195.80	6.37
	E_{ecdP}	A_{cdP}	212.00	6.37
Chemosorption in the growth area	E_{gaAs_2}	A_{gaAs}	0	6.00
	E_{gaP_2}	A_{gaP_2}	0	6.00

In the accepted approximation, the activation energy of the vacancy does not depend on which molecule is currently above the vacancy. The probability of reacting with an activated vacancy in molecules is less than one and may be different for different molecules. This is reflected in a certain difference in the values of A in the transition constants $As_2 \rightarrow DAs$ and $P_2 \rightarrow DP$.

6. CONCLUSION

A kinetic model of the composition formation in the anionic sublattice of the solid solution GaP_xAs_{1-x} at MBE on the vicinal surface (001) using As_2 and P_2 molecular fluxes is proposed. It differs from the model from [15] by taking into account non-stationary replacement processes occurring at the edges of terraces. The model is based on a two-dimensional layered growth mechanism, in which the terraces having a reconstructed surface are consistently completed in the growth areas localized in the fractures of the steps. Both atoms of the fifth group elements, which are included in the surface superstructure of the terraces as dimers, and atoms entering the growth region in the form of As_2 and P_2 molecules from the physisorbed state, are incorporated into the nodes of the anion sublattice of the crystal in the growth regions. The composition of the surface superstructure depends on the time of a single monolayer formation and the terrace edges renewal frequency. The growth time of one monolayer is a function of the growth rate. The frequency of updating of the edges of terraces depends on both the growth rate and the steps density (the magnitude of the substrate misorientation angle).

Elementary processes of mass transfer are considered in growth regions on the surface of terraces, as well as on their edges. By comparing the calculated values of the phosphorus fraction x with experimental data, the kinetic constants of the model were determined. The effect of the growth rate on x is due to the processes of the fifth group dimers transitions from SS to the molecular state and chemisorption of As_2 and P_2 molecules on the resulting vacancies on the edges and surface of terraces outside the growth areas. With a decrease in the growth rate, the composition of the solid solution shifts towards a higher proportion of phosphorus. The dependence of the composition of the solid solution on the substrate misorientation angle α is associated with the processes of transitions of the dimers of the elements of the fifth group from the

SS to the molecular state and the chemisorption of As_2 and P_2 molecules on the vacancies formed on the edges of terraces outside the growth regions. The proportion of phosphorus increases with increasing α.

The model allows an a priori assessment of the composition of a solid solution depending on the growth conditions, as well as the selection of molecular fluxes of the fifth group elements, ensuring the required composition of a solid solution at optimal values of temperature, growth rate, and superstructural state and the substrate surface misorientation angle. The model contains a number of approximations and assumptions. It does not explicitly take into account factors that may occur in real conditions, for example, chemisorption (desorption) of arsenic and phosphorus dimers into an out-of-structure position, as well as their diffusion in this state.

The possibility of localization of molecules in a physosorbed state during the DV → MV transition has not been discussed. Interlayer diffusion and the role of steps in this process are excluded from consideration. There is also no accounting for the influence of the elastic stress factor. Nevertheless, the model consistently describes the complex behavior of the phosphorus fraction in a solid solution in a fairly wide range of growth conditions, depending on J_{Ga}, J_{As_2}, J_{P_2}, T_s, V_g and α. This indicates the legitimacy of including in the consideration of the process of formation of the composition of solid solutions of $A^{III}B^{V}$ substitution for the fifth group of non- stationary processes on the growth surface.

FUNDING

The work was carried out with the support of the Ministry of Science and Higher Education (grant No.075–15–2020–797 (13.1902.21.0024)).

REFERENCES

1. S. Martini, A.A. Quivy, A. Tabata, and J.R. Leite, Vac. Sci. Techn. B18, 1991 (2000), doi: 10.1116/1.1303851.
2. R.K. Tsui, J.A. Curless, G.D. Kramer, and M.S. Peffley, Jpn. J. Appl. Phys. 58, 2570 (1985), doi:10.1063/1.335884.
3. Yu.B. Bolkhovityanov, O.P. Pchelyakov, UFN178, 459 (2008), doi: 10.3367/UFNr.0178.200805b.0459.
4. K. Mochizuki and T. Nishinaga, Jpn. J. Appl. Phys. 27, 1585 (1988), doi:10.1143/JJAP.27.1585.
5. J.R. Arthur, Surf. Sci. 43, 449 (1974), doi: 10.1116/1.1317818.
6. C.T. Foxon and B.A. Joyce, Surf. Sci. 64, 293 (1977), doi:10.1016/0039–6028(77)90273–4.
7. K. Ploog, Ann. Rev. Mater. Sci. 11, 171 (1981), doi:10.1146/annurev.ms.11.080181.001131.
8. J.M. Van Hove, P.J. Cohen, and J. Vac. Sci. Technol. 20, 726 (1982), doi: 10.1063/1.96017.
9. C.E.C. Wood, C.R. Stanley, G.W. Wicks, and M.B. Esi, J. Appl. Phys. 54, 1868 (1983), doi: 10.1063/1.332239.
10. Y.H. Wang, W.C. Liu, C.Y. Chang, and S.A. Liao, J. Vac. Sci. Technol. B4(1), 30 (1986), doi: 10.1116/1.583319.
11. T. Nomura, H. Ogasawara, M. Miyao, andM. Hagino, J. Crystal Growth 111, 61 (1991), doi: 10.1016/0022–0248(91)90947–4.
12. S. Yu. Karpov and M.A. Maiorov, Surf. Sci. 393, 108 (1997), doi: 10.1016/S0039–6028(97)00563–3.
13. E.S. Tok, J.H. Neave, F.E. Allegretti, J. Zhang, T.S. Jones, and B.A. Joyce, Surf. Sci. 371, 277 (1997), doi: 10.1016/S0039–6028(96)01085–0.
14. Yu.G. Galitsyn, S.P. Moshchenko, and A.S. Suranov, Phys. Low-Dim. Struct. 7/8, 81 (1998).
15. E.A. Emelyanov, M.A. Putyato, B.R. Semyagin, D.F. Feklin, V.V. Preobrazhensky, FTP 49, 163 (2015).
16. R. Heckingbottom, G.J. Davies, and K.A. Prior, Surf. Sci. 132, 375 (1983), doi: 10.1016/0039–6028(83)90548–4.
17. R. Heckingbottom, J. Vac. Sci. Technol. B3, 572 (1985), doi: 10.1116/1.583182.
18. H. Seki and A. Koukitu, J. Cryst. Growth 78, 342 (1986), doi: 10.1016/0022–0248(86)90070–9.
19. P.S. Kopyev, N.N. Lollipops, FTP 22, 1729 (1988).
20. S.V. Ivanov, P.D. Altukhov, T.S. Argunova, A.A. Bakun, A.A. Budza, V.V. Chaldyshev, Yu.A. Kovalenko, P.S. Kop'ev, R.N. Kutt, B. Ya. Meltser, S.S. Ruvimov, S.V. Shaposhnikov, L.M. Sorokin, and V.M. Ustinov, Semicond. Sci. Technol. 8, 347 (1993), doi: 10.1088/0268–1242/8/3/008
21. A.Y. Egorov, A.R. Kovsh, A.E. Zhukov, V.M. Ustinov, P.S. Kopyev, FTF 31, 1153 (1997), doi:10.1134/1.1187033.
22. V.V. Preobrazhensky, V.P. Migal, D.I. Lubyshev, Surface. Physics, Chemistry, Mechanics 9, 156 (1989).
23. V.V. Preobrazhensky, M.A. Putyato, B.R. Semyagin, FTP 36, 897 (2002).
24. Y. Tatsuoka, H. Kamimoto, T. Kitada, S. Shimomura, and S. Hiyamizu, J. Vac. Sci. Technol. B18, 1549 (2000), doi: 10.1116/1.591424.
25. C.T. Foxon, B.A. Joyce, and M.T. Norris, J. Gryst. Growth. 49, 132 (1980), doi: 10.1016/0022–0248(80)90073–1.
26. B.W. Liang and C.W. Tu, J. Appl. Phys. 72, 2806 (1992), doi: 10.1063/1.351532.
27. T. Shitara, D.D. Vvedensky, M.R. Wilby, J. Zhang, J.H. Neave, and B.A. Joyce, Phys. Rev. B46, 6825 (1992), doi: 10.1103/physrevb.46.6825.